J Inf Process Syst, Vol.15, No.1, pp.189~202, February 2019
https://doi.org/10.3745/JIPS.04.0104

ISSN 1976-913X (Print)
ISSN 2092-805X (Electronic)

JOURNAL OF INFORMATION PROCESSING SYSTEMS JIPS

Simulation Study on Measuring Pulverized Coal Concentration in Power Plant Boiler

Lijun Chen*, Yang Wang*, and Cheng Su*

Abstract

During thermal power coal-fired boiler operation, it is very important to detect the pulverized coal concentration in the air pipeline for the boiler combustion stability and economic security. Because the current measurement methods used by power plants are often involved with large measurement errors and unable to monitor the pulverized coal concentration in real-time, a new method is needed. In this paper, a new method based on microwave circular waveguide is presented. High Frequency Electromagnetic Simulation (HFSS) software was used to construct a simulation model for measuring pulverized coal concentration in power plant pipeline. Theoretical analysis and simulation experiments were done to find the effective microwave emission frequency, installation angle, the type of antenna probe, antenna installation distance and other important parameters. Finally, field experiment in Jilin Thermal Power Plant proved that with selected parameters, the measuring device accurately reflected the changes in the concentration of pulverized coal.

Keywords

Circular Waveguide, Concentration of Pulverized Coal, Firing Frequency, HFSS

1. Introduction

At present, China's total thermal power plant coal-fired boiler capacity is more than 200 GW, accounting about 70% of the entire installed capacity. Thus, thermal power is still in a dominant position. How to improve the efficiency of coal-fired boilers, accurately monitor the concentration of pulverized coal in primary air pipelines, and ensure pulverized coal fully burned in the boiler are among the most important research topics [1].

There are many methods to measure the concentration of pulverized coal in the primary air pipelines of a power plant, such as thermal balance method, pressure differential method, optical pulsation method, capacitance method. Thermal balance method to measure the concentration of pulverized coal requires the system in the adiabatic state before and after mixing. Measured results are affected if the condition is not meet [2]. For example, pressure loss during air and pulverized coal mixing process, pressure loss caused by the suspension of particles in the pipeline, and pipe resistance will reduce the measurement accuracy of thermal balance method. Optical pulsation method relies on expensive instruments, which are also hard to calibrate and operate. Therefore, it is difficult to popularize optical pulsation method in

Manuscript received April 3, 2017; first revision November 7, 2017; second revision December 22, 2017; accepted December 30, 2017.
Corresponding Author: Lijun Chen (1366523412@qq.com)
* The School of Automation Engineering, Northeast Electric Power University, Jilin, China ({1366523412, 913358948, suchg}@qq.com)

the power plants [3]. Capacitance method's sensitivity distribution is not uniform, and the measured results are also affected by the sudden change of pulverized coal concentration, distribution, and flow pattern, resulting in a large error. On the other hand, the new microwave circular waveguide method of measuring the concentration of pulverized coal, has attracted more and more attention from both the scientific research units and power plants because of its high precision, convenient measurement, simple replacement and high real-time property [4].

However, it is difficult to do experiments directly in the power plants, due to their operating conditions. Therefore, this paper used High Frequency Electromagnetic Simulation (HFSS) software to simulate the primary air pipeline of a power plant and study the parameters involved in the actual installation. Based on the simulation results, a measuring device was built and tested in a field experiment at Jilin Thermal Power Plant.

2. System Structure

Fig. 1 shows the principle model of boiler pulverized coal concentration system. Pulverized coal in coal feeder is fed into the boiler to combust through four primary air pipelines. The radius of each primary air pipeline is 0.3 m. Inside each primary air pipeline, a microwave transmitting probe and a receiving probe are installed, for a total of eight probes.

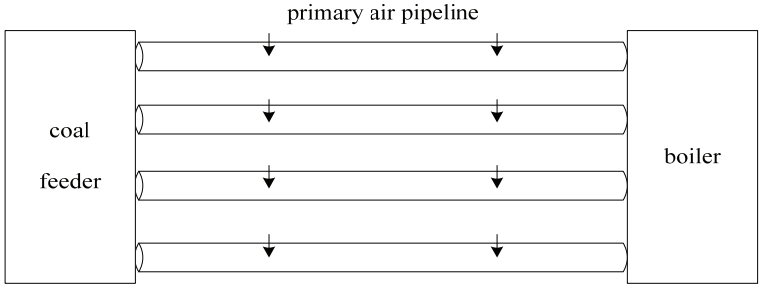

Fig. 1. The principal model of boiler pulverized coal concentration system.

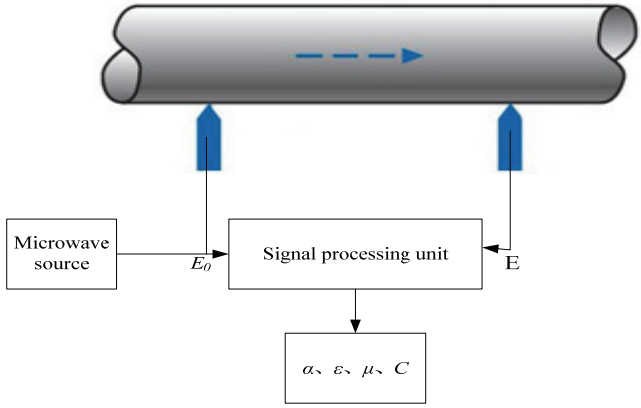

Fig. 2. Schematic diagram of pulverized coal concentration measurement.

Fig. 2 is a schematic diagram of the concentration measurement of pulverized coal in one of the primary air pipelines.

In the Fig. 2, E0 and E represent the microwave signal of the transmitting probe and the receiving probe. When the microwave propagates along the pipeline, the attenuation of the microwave signal and transmission loss A(P) [5] in the pipeline is:

$$\begin{cases} E = E_0 e^{-(\alpha+\beta)r} \\ \mathrm{A(P)db} = 10\lg(\mathrm{P_1}/\mathrm{P_0}) \end{cases} \tag{1}$$

where r is the microwave propagation distance, α is the attenuation constant, β is the phase constant, P_1 is received power of microwave, and P_0 is transmitted power of microwave.

Through calculation and analysis of transmission loss by the signal processing unit, and based on waveguide theory [6], α, ε, μ and coal concentration n can be obtained. In order to accurately measure the E_0 and E, HFSS is used to find the reasonable microwave emission frequency, the probe installation angle, the probe antenna type, installation distance and some other important parameters.

3. Selection of Waveguide Microwave Frequency

According to the relationship between the electromagnetic field and its direction of transmission, the wave transmitted in the circular waveguide can be divided into the transverse electric (TE) wave (the component of the electric field is 0 in the transmission z direction) and the transverse magnetic (TM) wave (the component of the magnetic field is 0 in the transmission z direction). According to the different cut-off frequency, the TE wave and TM wave can also be divided into a variety of modes [7].

According to the waveguide Maxwell's equations [6], for TE mode, H_Z equation can be obtained:

$$\nabla^2 H_Z + k^2 H_Z = 0 \tag{2}$$

where $k = \omega\sqrt{\mu\varepsilon}$, called the wave number of the medium. When $H_z(\rho,\varphi,z) = \hat{Z}H_Z(\rho,\varphi)$ is applied to the formula (2), the field component of the electric and magnetic field in the ρ,ϕ,z direction can be obtained. It's as follows:

$$\begin{cases} H_Z = A\sin\varphi J_n(k_c\rho)e^{-j\beta z} \\ E_\rho = \dfrac{-j\omega\mu}{k_c^2\rho} A\cos\varphi J_n(k_c\rho)e^{-j\beta z} \\ E_\varphi = \dfrac{j\omega\mu}{k_c} A\sin\varphi J_n'(k_c\rho)e^{-j\beta z} \\ H_\rho = \dfrac{-j\beta}{k_c} A\sin\varphi J_n'(k_c\rho)e^{-j\beta z} \\ H_\varphi = \dfrac{-j\beta}{k_c^2\rho} A\cos\varphi J_n(k_c\rho)e^{-j\beta z} \\ E_Z = 0 \end{cases} \tag{3}$$

where $J_n(x)$ is the first-class Bessel function, k_c is the cut-off wave number. When $E = E_{\varnothing} = 0$ and $\rho = a$, a is the radius of the circular waveguide, is applied to the E_{φ} equation, $J_n'(k_c a) = 0$ can be obtained at the conductor wall. The root of $J_n'(x)$ is defined as p_{mn}, it's the first m roots of J_N', then $p_{mn} = k_c a$. So there will be many k_c values, and k_c determines the cut-off frequency of the wave.

The cut-off frequency formula [8] of circular waveguide TE mode and TM mode is as follows:

$$f_{c_{nm}} = \frac{k_c}{2\pi\sqrt{\mu\varepsilon}} = \frac{p_{nm}}{2\pi a\sqrt{\mu\varepsilon}} \tag{4}$$

where k_c is the cut-off wave number, P_{nm} is the root of the first-class Bessel function, μ is the dielectric magnetic permeability, and ε is the dielectric permittivity of the medium. Since the TE11 mode is the main fundamental mode of all the transmission waves of the circular waveguide, it is possible to select the waveguide size and the operating frequency to be able to only transmit TE11 mode in the circular waveguide during the simulation.

In this study, the radius of the primary air pipeline of the power plant was 0.3 m, the cut-off frequency formula was (4), and the pulverized coal magnetic permeability μ was about 1, so we only need to know the dielectric constant ε of the pulverized coal and air mixture in the pipeline, then the cut-off frequency can be calculated. The relative permittivity of air is about 1, the relative permittivity of pulverized coal is about 2.7, and the formula for dielectric permittivity of mixture [9] is as follows:

$$\varepsilon = [m_1(\varepsilon_1)^{1/3} + m_2(\varepsilon_2)^{1/3}]^3 \tag{5}$$

where m_1 is the mass concentration of air, m_2 is the mass concentration of pulverized coal, ε_1 is the dielectric permittivity of air, ε_2 is the permittivity of pulverized coal, and the relationship between pulverized coal concentration and dielectric permittivity can be obtained:

$$m_2 = \frac{\varepsilon^{1/3} - 1}{2.7^{1/3} - 1}. \tag{6}$$

In the actual power plant operation, the pulverized coal concentration is generally between 0.2 kg/kg and 1.0 kg/kg [10], the dielectric permittivity ε is the maximum of 1.7. When there is only air in the pipeline, the cut-off frequency of the TE11 mode was about 292.83 MHz. The highest frequency mode closest to cut-off frequency of the TE11 mode is TM01 mode, whose cut-off frequency was 453.21 MHz. When there was only pulverized coal in the pipeline, the cut-off frequency of TE11 mode was 224.59 MHz, and the cut-off frequency of TM01 mode was 347.6 MHz. According to [11], in TE mode, TE11 mode had the lowest *P* value, 1.841, and TE21 model had the second lowest *P* value, 3.054. In TM model, TM01 model had the lowest *P* value, 2.405. Therefore, in order to ensure that there is only TE11 single-mode transmission in the pulverized coal pipeline, the microwave emission frequency must be greater than 292.83 MHz and less than 347.6 MHz. Thus, the frequency of microwave selected for this study was 300 MHz.

4. HFSS Model Parameter Setting

HFSS is a three-dimensional and high-frequency electromagnetic simulation software package designed by Ansoft Company in the United States. The software package is widely used in high frequency electromagnetic structure simulation, microwave component simulation and electromagnetic scattering problems [12].

4.1 Selection of Microwave Probe Antenna

Coaxial line is commonly used in microwave signal transmission line, and the specific formula [13] is as follows:

$$Z = \frac{60}{\sqrt{\varepsilon}} * In \frac{b}{a} \tag{7}$$

where b is the coaxial outer diameter, and a is the coaxial inner core diameter, and ε is the dielectric permittivity of the coaxial filling medium. To minimize the loss of microwave signals, the filling medium chosen in this paper is air. The outer and inner core diameter largely affect the power capacity and loss of the coaxial line during transmission. According to [14], when b/a = 1.649, the coaxial line has the largest power capacity, with the characteristic impedance of the coaxial line equals to 30, but the loss is large; when b/a = 3.6, the loss of the coaxial line is minimal, the characteristic impedance of the coaxial line is 76.7 Ω, but the power capacity of the coaxial line is small. The maximum transmission capacity and the minimum attenuation is generally impossible to meet at the same time, in order to take into account of both values, the suitable size is b/a = 2.3, so the characteristic impedance of the coaxial line is 50 Ω, at this time, the power capacity is less about 15% than the best case, while the attenuation is greater about 10% than the best case.

This model selects a quarter-wavelength monopole antenna as the system's transmitting and receiving antenna. The input impedance of the monopole antenna is close to 50 Ω [15] and can be directly matched with a coaxial line with a characteristic impedance of 50 Ω .

The probe model shown in Fig. 3 uses coaxial line feed, length = 0.24 m [16] and coaxial diameter ratio b/a = 2.3. This ensures that the antenna and coaxial impedance can match. Besides, a ceramic protective sleeve that does not interfere with the microwave is provided outside the antenna to protect the antenna from being pulverized.

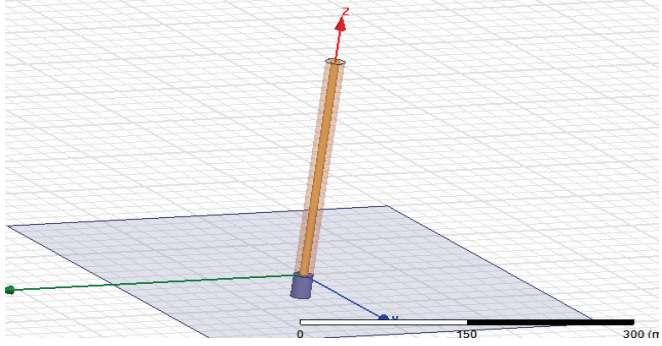

Fig. 3. HFSS model of monopole antenna.

In the antenna design, the return loss is an important parameter, and the return loss is the signal reflection of performance parameters. The return loss indicates the portion of the incident power reflected to the signal source. In practical applications, it is desirable that the as much as possible microwave wave is transmitted, that is, no echo is desired. The simulation result of the monopole antenna is shown in Fig. 4.

It can be seen from Fig. 4, there was a maximum absolute value of return loss (RL) around the 300 MHz frequency band, its value was about 25 dB, meeting the general antenna design requirements. This is also consistent with the microwave frequency calculated in the second section, which proves that 300 MHz is a suitable microwave frequency to use in this study.

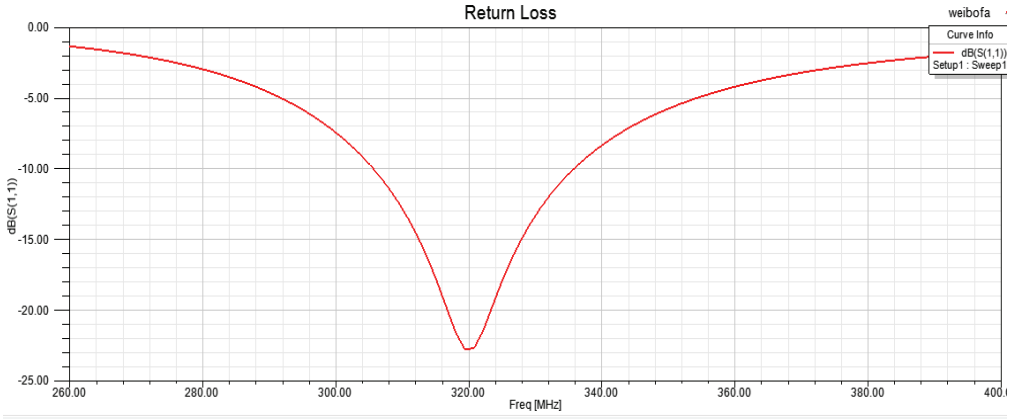

Fig. 4. Antenna return loss.

4.2 Microwave Probe Antenna Installation Location

Through the antenna radiation pattern, we can calculate the microwave gain strength. The HFSS can plot the three-dimensional space of the antenna and the field intensity drawing of the two-dimensional plane. Radiation direction is shown in Fig. 5.

It can be seen from Fig. 6 that the monopole antenna has the maximum gain in the horizontal direction, so the angle of the transmitting probe and the receiving probe should be placed parallel to ensure the largest transmission of the microwave signal.

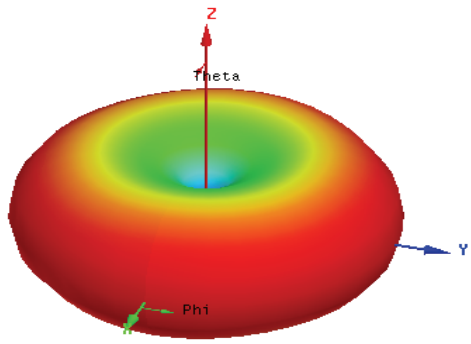

Fig. 5. Three-dimensional field strength direction.

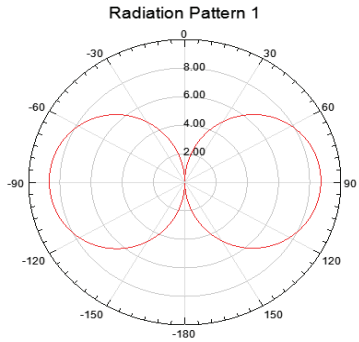

Fig. 6. E surface (YOZ surface) field strength direction.

4.3 Simulation Model of Microwave Measurement Concentration

The primary air pipeline was made of iron, with radius = 0.3 m, length = 2 m. Microwave frequency used in this experiment was 300 MHz. Transmitting and receiving probes were placed parallel to the inside of the pipe, and the model was established as shown in Fig. 7.

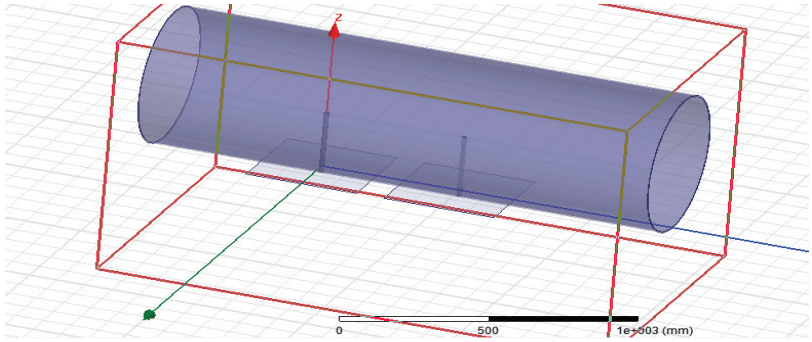

Fig. 7. Experimental model of microwave concentration measurement.

After the microwave frequency and the position of the probe were determined, the change of the pulverized coal concentration of the primary air pipeline was simulated by changing the dielectric constant of the pipeline. The influence of probe distance on the measurement of pulverized coal concentration was investigated.

As above, we can see the pulverized coal concentration in the operation of the power plant is generally within the range of 0.2 kg/kg to 1.0 kg/kg, so the two groups with dielectric constant between 1.4 and 1.7 were selected, corresponding to the pulverized coal concentration of 30% and the pulverized coal concentration of 50%. Changed the distance between transmitting and receiving probes and observed the attenuation of the probe transmission.

When the probe was separated by 0.1 m and the dielectric permittivity of the piped mixture was 1.4 and 1.7, the simulation results were shown in Fig. 8.

Two curves shown in Figs. 8 and 9 are S_{11} (red) and S_{21} (purple). S_{11} curve represents the return loss, and S_{21} curve represent the transmission coefficient, the transmission loss between the probes. It can be seen from Figs. 8 and 9, when the two probes are separated by 0.1 m and the pulverized coal concentration

was 30%, the transmission loss between the probes was -2.02 dB and the receiving power was about 63% of the transmit power. When the coal concentration was 50%, the transmission loss between the probes was -1.93 dB and the power of the receiving probe was about 64% of the transmit power, varying by 1%. This indicates that the distance between the probes was too close and needed to be increased. Further experiments with increased distance were done, and the difference between the transmission loss of the 30% and 50% pulverized coal concentration were plotted. The results are shown in Fig. 10.

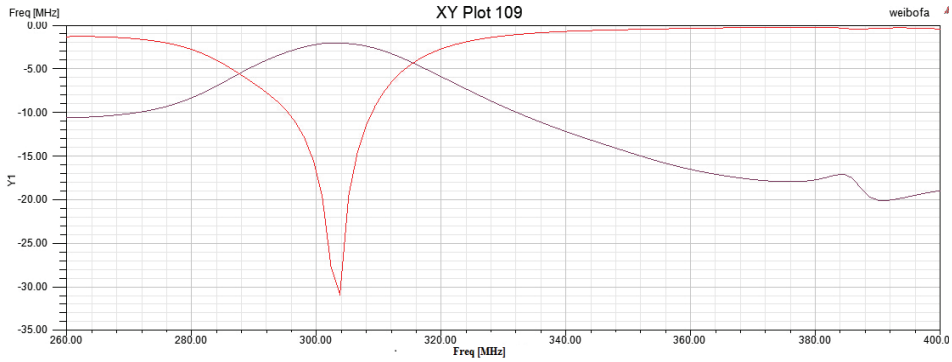

Fig. 8. Dielectric constant = 1.4.

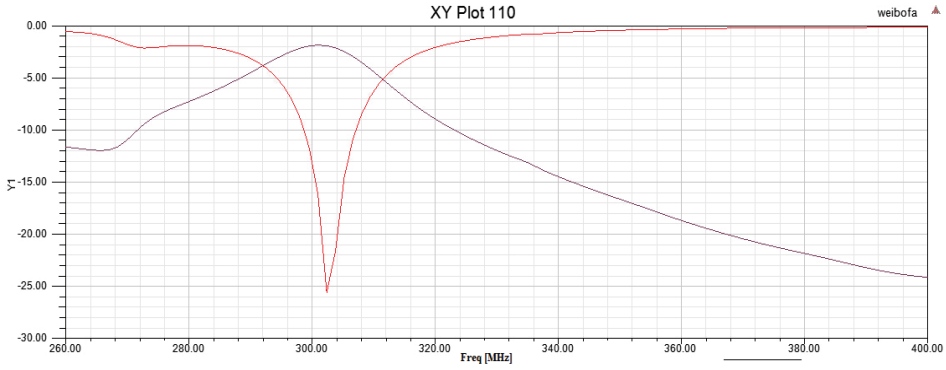

Fig. 9. Dielectric constant = 1.7.

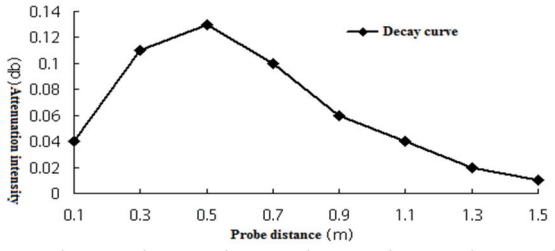

Fig. 10. Decay curve.

It can be seen from Fig. 10, when the probes were close from each other, the microwave signal was received by the receiving probe without sufficient attenuation, resulting in insensitivity for changes in the concentration of pulverized coal. When the probes were placed far away, the signal from the transmitting

probe to the receiving probe was only a fraction of the original signal. The attenuation caused by the change in the pulverized coal concentration was also reduced. When the probe distance was in the vicinity of 0.5 m, the attenuation had the maximum rate of change, so 0.5 m is the best microwave probe installation distance in this experiment.

5. Experimental Results

According to the HFSS results, the pulverized coal concentration measuring device was installed in the primary air pipeline of the Jilin Thermal Power Plant. The system was composed of microwave antenna, data acquisition system, host computer and other accessories. During actual measurement, 2/3 of microwave antenna was inserted into the primary air pipeline (Fig. 11).

The device was tested in four conditions as below: start the powder feeder, stop the powder feeder, adjust the rotational speed of the powder feeder, and adjust air damper opening degree. The device measurements were compared with the amount of pulverized coal supplied in four cases.

Fig. 11. On-site installation diagram of pulverized coal on-line measurement system.

5.1 Start the Powder Feeder

Fig. 12 shows the wind speed and the rotational speed of the powder feeder were measured by the detection device and the backrest tube for a period of time before and after the start of the powder feeder.

In Fig. 12, the upper curve shows the concentration of pulverized coal detected by the device. The lower curve shows the wind speed and the rotational speed of the powder feeder measured by the backrest tube and recorded by the power plant DCS system. As seen from the figure, the powder feeder started at 14:50:02, and the device detected a step of coal concentration at 14:50:16. The delay time detected by the device is the time required for the pulverized coal to reach the probe sensor in the primary air pipeline when the powder feeder was just started.

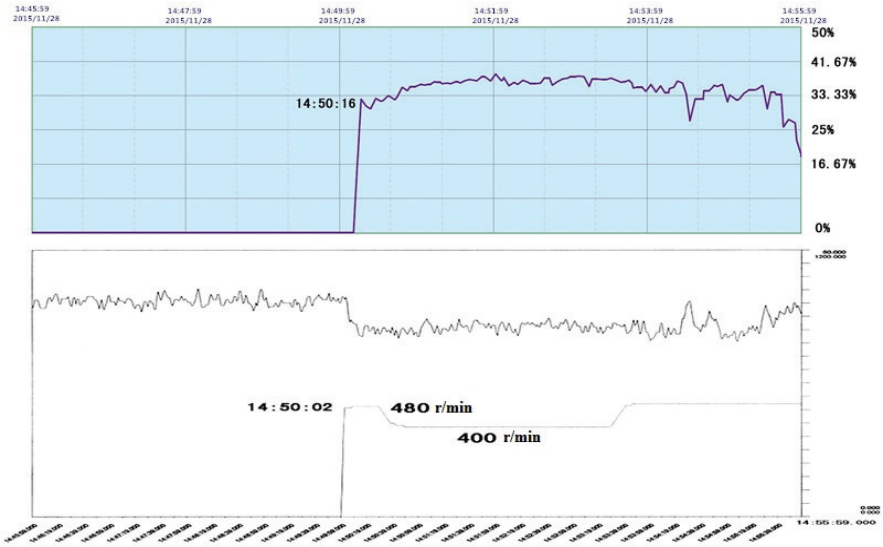

Fig. 12. Device measurement curve and DCS display curve when powder feeder is started.

5.2 Stop the Powder Feeder

Fig. 13 shows both the wind speed and the rotational speed of the powder feeder, which were measured by the detection device and the backrest tube for a period of time before and after the stop of the powder feeder. The upper curve is the pulverized coal concentration detected by the device. The lower curve is the wind speed and the rotational speed of the powder feeder measured by the backrest tube, which was recorded by the power plant DCS system.

It can be seen from Fig. 13, the powder feeder started at 15:06:24, and the device detected that the pulverized coal concentration dropped rapidly and dropped to zero at 15:06:35. The delay detected by the device was the time required for the pulverized coal to stop in the primary air pipeline when the powder feeder was stopped.

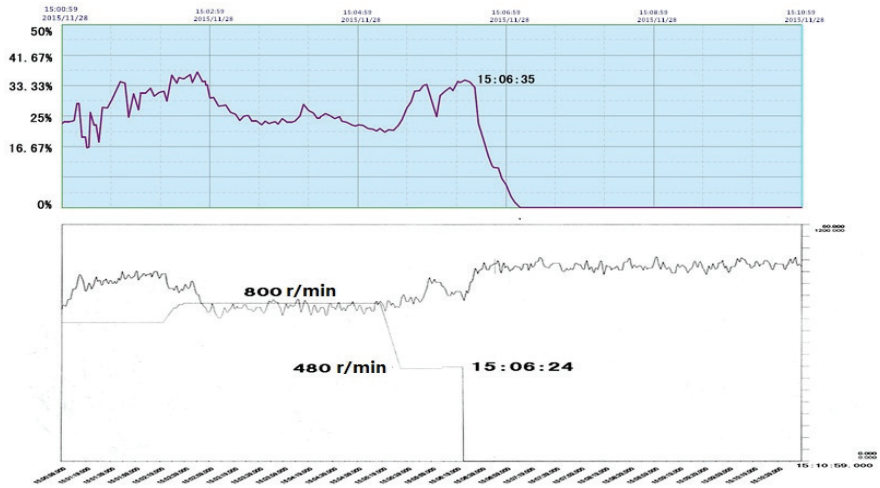

Fig. 13. Device measurement curve and DCS display curve when powder feeder is stopped.

5.3 Adjust the Rotational Speed of Powder Feeder Separately

We adjusted the powder feeder separately and increase the rotational speed of the powder feeder from 400 r/min to 800 r/min, then observed value variation measured by the detection device on the concentration of pulverized coal. As shown in Fig. 14, the upper curve is the concentration of the pulverized coal and the velocity of flow of the pulverized coal detected by the device. The lower curve is the wind speed and the rotational speed of the powder feeder measured by the backrest tube and recorded by the power plant DCS system.

As seen from Fig. 14, due to the non-linear relationship between the rotational speed of the powder feeder and the amount of powder supplied, the concentration of pulverized coal had a small increase. And during the increase of rotational speed of the powder feeder from 400 r/min to 600 r/min, the velocity of flow of the pulverized coal measured by the device and the wind speed measured by the backrest tube were also experienced a small decreased. Between 600 r/min and 800 r/min, the pulverized coal concentration increased significantly, and the velocity of flow of the pulverized coal measured by the device and the wind speed measured by the backrest tube were also significantly decreased. This shows that the speed and concentration measured by the device can reflect the change in pulverized coal supply.

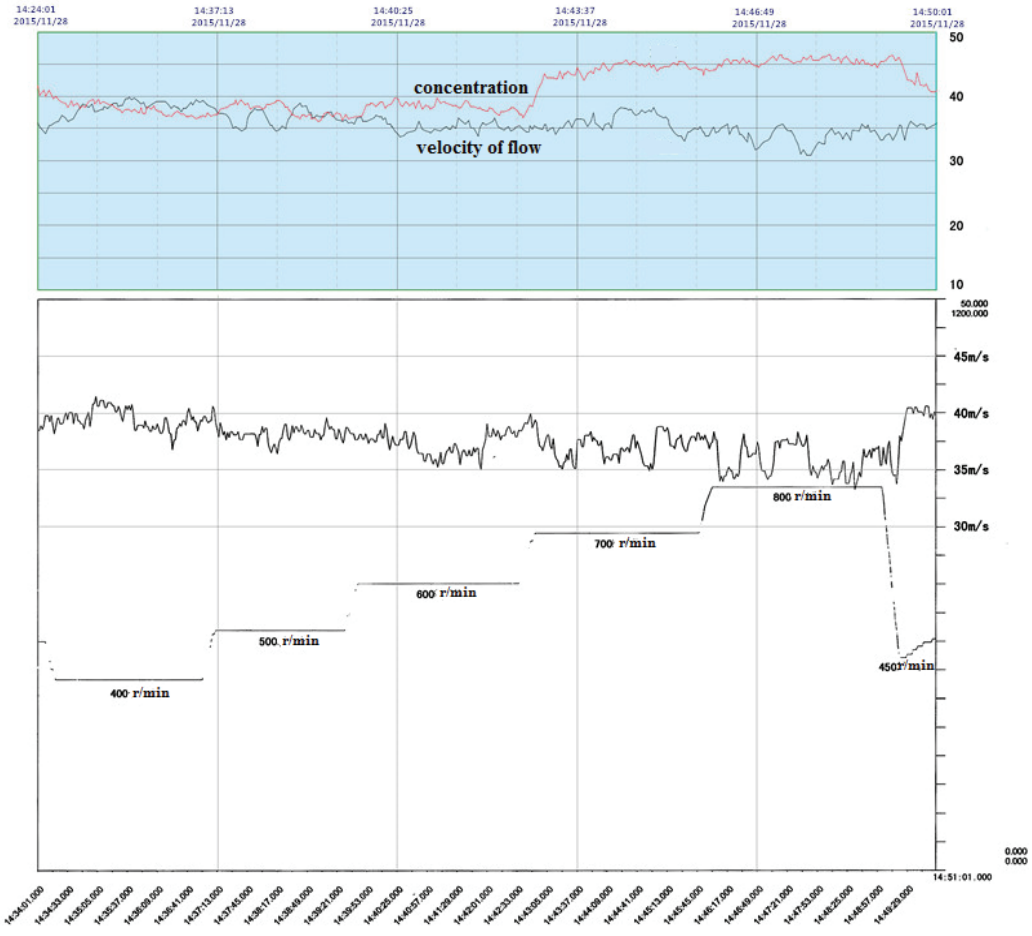

Fig. 14. Concentration curve when adjusting the rotational speed of the powder feeder.

5.4 Adjust Air Damper Opening Degree Separately

Fig. 15 shows the variation of concentration when air damper opening degree was changed. It can be seen from the figure, at 10:40, air damper opening degree decreased from 100% to 80%, the velocity of flow of the pulverized coal decreased slightly. At 10:44, air damper opening degree decreased from 80% to 50%, the velocity of flow of the pulverized coal dropped significantly to 25 m/s or so. At this time, the pipe was slightly blocking, so the pulverized coal concentration was also declining. At 10:48, the experimental operators showed the wind speed was too low, and increase air damper opening degree from 50% to 100%. Since then, the velocity of flow of the pulverized coal began to increase, and the concentration of the pulverized coal began to decreased rapidly and then increased again, which proved the pulverized coal blocking the pipe had been blown off at that time (Table 1).

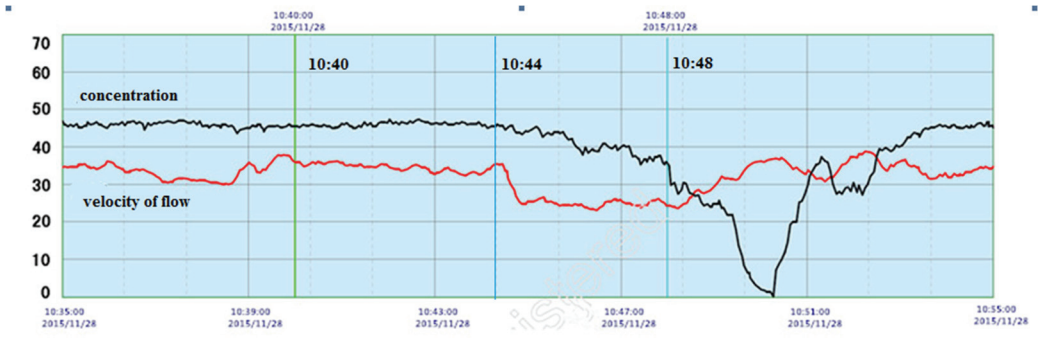

Fig. 15. Monitoring curve when adjusting air damper opening degree.

Table 1. Air damper opening degree records

Time (March 5, 2016)	Opening degree (%)
At the start of the experiment	100
10:40–10:44	80
10:44–10:48	50
At the end of the experiment	100

From Figs. 12–15, it can be seen that the microwave circular waveguide method of measuring the pulverized coal concentration well reflect the changes of pulverized coal concentration during boiler normal operation. The results showed that the microwave transmission frequency, probe mounting angle setting, antenna probe selection, probe distance, and other parameters were set reasonable and successful. At the same time, it suggests that the method presented in this paper can be used in real settings to measure the concentration of pulverized coal, solving the series problems shared by the traditional measuring methods.

6. Conclusion

The HFSS provides effective guidance for the microwave transmission frequency, probe mounting angle, antenna probe selection and probe distance for the detection device. Based on the simulation

results, important parameters were chosen, and the device was tested in actual field study. Comparing the measured results from the device and the power plant DCS system, it can be concluded that the device measurement can accurately reflect the concentration of pulverized coal. This study also shows that the HFSS greatly saves the development period of the measuring device.

Acknowledgement

This study is supported by the Jilin Province key scientific and technological transformative project (No. 20150307003GX) and the Youth Science Fund Project (No. 61304013).

References

[1] W. G. Pan and J. M. Cao, "Study on techniques for online measurement to air and pulverized coal mixture flow parameters of coal-fired boiler in power plant," *Proceedings of the CSEE*, vol. 24, no. 10, pp. 193-195, 2004.

[2] J. Ma and Y. Yan, "Design and evaluation of electrostatic sensors for the measurement of velocity of pneumatically conveyed solids," *Flow Measurement and Instrumentation*, vol. 11, no. 4, pp. 195-204, 2000.

[3] Y. Yan and A. R. Reed, "Experimental evaluation of capacitance transducers for volumetric concentration measurement of particulate solids," *Flow Measurement and Instrumentation*, vol. 10, no. 1, pp. 45-49, 1999.

[4] X. S. Cai, Y. Z. Pan, X. Ouyang, W. L. Wu, J. Yu, and J. Hu, "The study of diagnosing the running condition of pulverized coal in pipe," *Proceeding of the CSEE*, vol. 21, no. 7, pp. 83-86, 2001.

[5] Y. X. Shi, D. B. Ge, and J. Wu, "Theoretical analysis of microwave attenuation constant of weakly ionized dusty plasma," *Chinese Journal of Geophysics*, vol. 50, no. 4, pp. 877-883, 2007.

[6] S. H. Shuo. *Microwave Technology Foundation*. Beijing: Higher Education Press, 2011.

[7] C. Q. Jiao and J. R. Luo, "Propagation of electromagnetic wave in a lossy cylindrical waveguide," Acta Physica Sinica, vol. 55, no. 12, pp. 6360-6367, 2006.

[8] Z. Y. Zhang, L. Z. Zhou, and D. M. Wu, *Microwave Engineering*, Beijing: Publishing House of Electronics Industry, 2006.

[9] J. H. Li, "Study of the electrical conductivity and dielectric constant of mixture," *Chinese Journal of Geophysics*, vol. 39, no. S1, pp. 364-370, 1996.

[10] L. Liu, H. S. Shao, F. D. Zhou, and D. Y. Wu, "Concentration measurement with thermal probe for pulverized coal in the pneumatic pipeline of power plant," *Flow Measurement and Instrumentation*, vol. 45, pp. 225-232, 2015.

[11] C. H. Liang, Y. J. Xie, and B. R. Guan, *Concise Microwave*. Beijing: Higher Education Press, 2006.

[12] C. Y. Dai, J. Y. Cai, Y. Y. Chen, Y. Zu, L. J. Lin, Y. L. Huang, and M. Yan, "Design and HFSS simulation of 13.56 MHz RFID reader antenna," *Radio Engineering*, vol. 2013, no. 1, pp. 42-45, 2013.

[13] J. F. Dong and S. J. Xu, "Reflection and transmission of coaxial waveguide partially filled with chiral media," *Journal of Infrared and Millimeter Waves*, vol. 21, no. 5, pp. 356-360, 2002.

[14] C. Bao and S. L. Wang, "The impedance and radiation characteristics of slanted slot on the shell of line," *Chinese Journal of Radio Science*, vol. 18, no. 3, pp. 317-320, 2003.

[15] H. S. Yang, F. L. Xie, and Z. F. Qian, "Study on input impedance of coaxial-line probe exciting circular waveguide," *Journal of Microwaves*, vol. 20, no. 1, pp. 58-60, 2004.

[16] A. S. Zhu, Z. L. Chen, and X. Q. Liu, "Numerical calculation of radiation characteristic of monopole and dipole antenna," *Journal of Microwaves*, vol. 31, no. 2, pp. 33-38, 2015.

Lijun Chen https://orcid.org/0000-0002-1344-8803

He received the Ph.D. degree in thermal engineering from North China Electric Power University in 2010. Since 2000, he is with the School of Automation Engineering from Northeast Electric Power University as a professor. His current research interests include detection of thermal process parameters in thermal power plant.

Yang Wang https://orcid.org/0000-0003-4636-4654

He received B.S. degree in school of automation from Qingdao Institute of Technology in 2015. Since September 2015, he is with the School of Automation Engineering from Northeast Electric Power University as a M.S. candidate.

Cheng Su https://orcid.org/0000-0001-7014-8463

He received the B.S. degree in thermal engineering from Heze University in 2015. Since September 2015, he is with the School of Automation Engineering from Northeast Electric Power University as a M.S. candidate.